Bioscene

Bioscene
Volume- 22 Number- 02
ISSN: 1539-2422 (P) 2055-1583 (O)
www.explorebioscene.com

Supervised Classification of Satellite Imagery to Produce the Land-Use and Land-Cover Information of Nigeria

Thomas U. Omali[1], Raphael I. Ndukwu[2], Sylvester. M.B. Akpata[3], Kebiru Umoru[4], John I. Ekele[5], Joseph N. Owan[6], Emmanuel W. Adekyeye[5], Temitope O. Ogunleye[6], Francis I. Okeke[2]

[1]National Biotechnology Development Agency (NABDA), Nigeria

[2]Department of Geoinformatics and Surveying, University of Nigeria Enugu Campus, Nigeria

[3]Department of Geoinformatics and Surveying, University of Abuja, Nigeria

[4]National Centre for Remote Sensing Jos, Nigeria

[5]Doctoral Candidate, Department of Geogeography, Nasarawa State University, Keffi, Nigeria

[6]Department of Geoinformatics and Surveying, University of Calabar, Nigeria

Corresponding Author: **Thomas U. Omali**

Abstract: Land use and land cover (LULC) products are important for comprehending anthropogenic interactions with the environment. The precise information about LULC of our environments is essential for various applications such as the monitoring and management of natural resources, producing development plans, and global change assessments. Regrettably, recent wall-to-wall LULC maps and statistics of Nigeria are not available. This work presents the spatiotemporal wall-to-wall LULC maps and estimates of Nigeria for 2000, 2010, and 2020.The study used 6 LULC classes in he classification process. The supervised classification was used to classify the LULC in the satellite imageries. With ground-truthing, the accuracy of the classification was also evaluated and validated.From the classification result, the grassland revealed the highest percentages throughout the time series as compared to other classes of LULC. It recorded the highest rate in 2010 at 28.06%. The LULC classification accuracy assessment result for 2000, 2010, and 2020 showed overall accuracies of 94%, 91%, and 95% respectively. Similarly, the kappa coefficients were 0.93, 0.89, and 0.94, correspondingly. There is significant variability regarding LULC in Nigeria. The fluctuations in the LULC implied both gain and loss in the LULC throughout the study epochs. The levels of accuracy obtained in the classification are highly acceptable as they are higher than 85% stipulated as the minimum accuracy required for research of this nature. Furthermore, the kappa coefficients indicate an almost perfect correlation between the classified pixels and ground-truth data.

Keywords: Anthropogenic, classification, global change, LULC, satellite imagery.

Introduction

Land use/Land cover (LULC) is essential for understanding the interactions of human activities with the environment (Ojha et al., 2013). It influences the ecosystem's role at all spatial scales (Song et al., 2018; Peters et al., 2019). The LULC pattern of a region is an

outcome of natural and human-induced factors (Mohammed et al., 2013; Shah et al., 2017). In other words, the alteration in LULC characteristics is usually regulated (Hurtt et al., 2011) by several socio-economic and biophysical elements (Shah et al., 2017; Popp et al., 2017) such as modifications in population, climate (Mohammed et al., 2013; IPCC, 2014), agronomic food demand (Alexandar et al., 2016), and others. Generally, the natural causes of LULC change may differ– varying from a gradual transformation at a time or a sudden disastrous occurrence at different extents and times.

Urbanization is a major driver of LULC alterations due to land utilization foressential infrastructure. Converting land from one LULC class to another is necessary for building roads, houses, railways, and airports, etc. Also, agricultural land expansion is a primary source of LULC change and deforestation. Furthermore, mining is very intensive and destructive. If it occurs in forest areas, it involves removing substantial trees both at the extraction of minerals and creation of access road. Similarly, deforestation worsens with wood as fuel in mining operations. Besides, mining activity encourages development that may cause population growth with resulting deforestation. Deforestation may arise due to untenable logging (Houghton, 2005). Sufficient evidence exists that the entire world is facing an ecological crisis due to heavy deforestation or LULC transformation. Thus, monitoring land modification is essential for evaluating global change impact on land and the consequence of land change on the ecosystem (Foley et al., 2005; Turner, Lambin, and Reenberg, 2007; Güneralp and Seto, 2013). By and large, the assessment of land alteration is a function of available classified spatial information supported by auxiliary variables (Verburg et al., 2015; Heck et al., 2018).

Nigeria is known for heterogeneous landscapes and complex land change processes, which may be linked mainly to cropland expansion, urbanization, and industrialization, etc. Regrettably, interest in studying country-wide LULC and its change is still very low in Nigeria. The available record indicates that only two major nation-wide LULC studies are available. The Nigeria RaDAR (NIRAD) project of 1976/78 offered the first national land use/land cover information. Yet, it has certain shortcomings (see Adeniyi, 1984; FORMECU, 1996). The second attempt to assess the LULC and vegetation in Nigeria was by the Forestry Management and Coordinating Unit (FORMECU) in 1996. The FORMECU project affords an update of the database created through the NIRAD project. However, evidence in the literature suggests that products from the FORMECU has its own flaws. Above all, both products and most maps used in Nigeria are obsolete. The implication is that any decision based on those maps will not reflect the current realities. Thus, there is an urgent need to update the wall-to-wall LULC map and estimate of Nigeria.

Many methods, such as the satellite-based and conventional terrestrial mapping are frequently used for spatiotemporal mapping of LULC. The terrestrial mapping is generally a labor-intensive, time-consuming and money-demanding method of mapping vast areas. It is however a direct mapping technique that can produce maps at various scales and degrees of precision. Also, subjectivity may be present in mapping based on ground or field method. Nevertheless, mapping LULC using satellites and aerial photography is more economical, time-efficient, spatially extensive, and multi-temporal. In the past, satellite data had a relatively lower spatial resolution than maps created by terrestrial surveys. Satellites

now offer data at multiple spatial and temporal scales using remote-sensing technology (Scaioni et al., 2014). Compared to other techniques like ground surveys, remote sensing offers the chance for rapid acquisition of LULC information at a significantly lower cost (Chen and Wang, 2010). For LULC mapping, satellite images provide high spatial coverage and multi-temporal product (Wittke et al., 2019; Viana, Girão, and Rocha, 2019).

Recently, there has been a lot of interest in using Machine Learning on remotely sensed imagery for LULC mapping (Adam et al., 2014; Maxwell, Warner, and Fang, 2018). Two subtypes of machine learning techniques have been identified, including supervised and unsupervised. Common examples of supervised classification techniques are Support Vector Machines (SVM), Random Forests (RF), Spectral Angle Mappers (SAM), Maximum Likelihood Classifiers (MLC), fuzzy logic, and others. Furthermore, some examples of unsupervised classification techniques are fuzzy c-means algorithms, K-means algorithms, and ISODATA (iterative self-organizing data) (Lambin, Geist, and Lepers, 2003). Recent research in land use and land cover classification has attracted more sophisticated methods such as ANN, SVM, RF, and others. As a result, a lot of research has been done on LULC modeling using various machine-learning (Teluguntla et al., 2018; Zhang et al., 2019) and comparing them (Li et al., 2016; Camargo et al., 2019). Employing remote sensing coupled with Geographic Information System is a powerful tool for analysis and visualization (Rekha et al., 2017).

It is clear how important it is to have accurate information about LULC and how it is changing in different endeavorus. Because of its wide spatial coverage and multi-temporal availability, satellite data have shown greater benefits in that regard (Wittke et al., 2019). In the application of Machine Learning to extract thematic information from satellite data, the supervised algorithms are common methods (van Leeu-wen, Tobak, and Kovács, 2020). For example, Balázs et al (2018) extracted data from Landsat 7 using Random Forest and Support Vector Machine and achieved overall accuracies of over 90%. Also, van Leeuwen, Tobak, and Kovács (2020) detected the LULC classes with inland excess water signified by two water classes. In the process, they compared the results of SVM, RF and a deep ANN based on overall accuracy and Cohen's Kappa. In a similar study, Abbas and Jaber (2020) used WorldView-2 imagery to produce the land use classification in Hilla city, Babylon, Iraq through a comparison among different algorithms. They also employed the Support Vector Machine and Maximum Likelihood. The result revealed that the Support Vector Machine method has the most significant overall accuracy equal to 94.48% with kappa co-efficient equal to 0.90. Of course, these values are much better and higher than those of Maximum Likelihood algorithm in estimating and extracting Land cover/Land use. Yousefi et al. (2011) mapped the LULC in Iran's Mazandaran province using Landsat ETM+. They evaluated nine distinct supervised classification techniques: binary code, minimum distance, spectral information divergence, neural network, spectral angle mapper, maximum likelihood, SVM, mahalanobis distance, and parallelepiped. According to the results, the SVM classifier outperforms the other classifiers in terms of accuracy. Like many previous LULC studies, we created the LULC map of Nigeria using Geographic Information System (GIS) and satellite remote sensing at 10-year intervals between 2000 and 2020.

Objectives

The broad aim of this work is to carry out the spatiotemporal mapping and estimation of the wall-to-wall LULC of Nigeria for 2000, 2010, and 2020. The specific objectives include

i. LULC classification of satellite data
ii. LULC classification accuracy assessment
iii. LULC change detection

Data and Methods

Study location

Nigeria is in the western region of Africa between latitudes 04°N and 14°N of the Equator and longitudes 03°E and 14°E of the Greenwich Meridian. It occupies an area of 923,768km^2, of which water bodies cover 13,000 km^2 while physical land covers 910,768km^2. Geographically, Nigeria shares common boundaries with Niger to the north, Chad and Cameroun to the east, the Atlantic Ocean to the south, and the Republic of Benin to the west. The country's total land boundaries are 4,047km in length, comprising 1,497km with the Niger Republic, 87km with Chad, 1,690km with Cameroun, and 773km with Benin. Nigeria's coastline spans over 853km, with the Niger Delta portion covering about 80% of the entire coastal length. The use of Nigerian landmass is such that 15% is for pastures, 10% for forest reserve, 10% for settlements, and the remaining 30% is considered uncultivable for various reasons (Federal Ministry of Environment, 2001).

Nigeria operates a Federal system of government with one stable central government, 36 states and a Federal Capital Territory (FCT). The States (and FCT) are subdivided into 774 Local Government Areas (and Area Councils) for grassroots administration. Furthermore, six geopolitical zones cover the 36 States (North–West, North–Central, North–East, South–East, South–South, and South–West) mainly for political purposes. Also, Nigeria is the most populous country in Africa. Information from the National Bureau of Statistics indicates that Nigeria's population as of 2020 was 206,152,701. A major number of people in this population dwell in the urban centers. Urbanization in Nigeria is influencing LULC change with its main impact being deforestation and forest degradation.

Nigeria also has two seasons—the dry and the wet. It is also characterized with a tropical climate with comparatively high temperatures. In the far south, the average maximum temperature is 32°C, whereas in the north, it is 41°C. The south's average minimum temperature is 21°C, while the north's is less than 13°C. Nigeria receives 500 mm of rainfall in the north and 4,000 mm in the southeast each year. Nigeria's coastal and southeast regions receive a lot of rainfall, which leads to the growth of rainforests there. The northern portion, on the other hand, experiences less rainfall and features progressively drier vegetation zones. Nigeria is also home to a variety of physiographical units and climatic regimes, which result in a wide range of ecological zones. Semi-arid, dry sub-humid, sub-humid, humid, extremely humid, ultra-humid (flood), mountainous, and plateau are all included in this. The savanna (Sahel, Sudan, Guinea, and Derived), lowland rainforest, freshwater swamp forest, mangrove forest and coastal vegetation, and montane forest zone are the five zones that can be streamlined due to their similar characteristics.Montane, freshwater and saltwater swamp, mangrove, rain forest, Guinea

savanna, Sudan savanna, and Sahel savanna are the seven major, discrete zones into which Nigeria's vegetation can be divided. Nigeria's coastline is home to both freshwater and saltwater swamps. The tropical lowland rainforest, a dense evergreen vegetation of tall trees with an undergrowth of small trees, shrubs, and herbs, replaces the mangroves along the lagoons. Nigeria's largest vegetation belt is the Guinea savanna. It is made up of both grass and trees, with trees predominating in areas with sparse populations. Regrettably, the progressive decline in Nigeria's forest over the past few decades poses extreme pressure on the conservation of its wild biotic resources as it continues to experience a loss of natural habitats (Okeke and Omali, 2016). For instance, northern Nigeria suffers a high rate of overgrazing and clearance of trees for firewood, while southern Nigeria suffers from logging.

The early post-independence (the early 1960s) economy of Nigeria was based on agriculture as demonstrated by its contribution to the GDP, and employment opportunities. Though the oil sector is now the most significant source of the national revenue, nearly 60% of the labour force in the country is engaged in agriculture. Furthermore, agriculture is the basis of resources used in the processing industries and a major source of the country's foreign earnings. The core of Nigeria's agricultural policy is self–sufficiency in fundamental commodities, especially those that it has proportional benefits in local products such as tuber crops (Soludo, 2006). The agricultural sector is likely to retain its relative dominance in terms of the total labour force for the economy of the country for a long time. Consequently, more forests and savanas are likely to be converted for agricultural use in the future.

Input data

The MODIS (Moderate Resolution Imaging Spectroradiometer) imagery was used in this study. The MODIS is onboard the Terra (EOS AM–1) and Aqua (EOS PM–1) plat-forms, launched on December 18th, 1999 and May 4th, 2002 respectively (Barnes, Xiong and Salomonson, 2003). The timing of Terra and aqua as the orbits the Earth is such that in the morning, Terra crosses the equator from north-south, and aqua crosses the equator from south to north in the afternoon. MODIS instrument provides 36 spectral bands ranging in wavelength from 0.46 μm to 14.4 μm (Masuoka et al., 1998). Also, MODIS has four refractive objective assemblies, one for each of the Visible (VIS), near-infrared (NIR), shortwave and mid-wave infrared (SWIR/MWIR), and longwave infra-red (LWIR) spectral regions (Ardanuy, Han, and Salomonson, 1991). MODIS has a swath width of 2,330km across the track by 10km along the track at the nadir. Of course, this exists over the sensor viewing angles of ±55° cross-track and the effective view angle on the ground being slightly larger owing to the Earth's curvature.

This study employed the MOD13A1 Version 6 product with a 16-day compositing period, which offers Vegetation Index (VI) values at a per-pixel basis of 500m spatial resolution. The four tiles of MODIS 13A1 datasets that covers Nigeria used in this analysis were from the NASA website (www.earthdata.nasa.gov). The application of MODIS data in diverse areas may be attributed to two important reasons. First, it is characterized by daily and high-quality data covering large areas of land. Second, it offers a good prospect for

monitoring and analyzing regional land surface processes. This is especially true for NDVI vegetation analysis, for which MODIS provides a standard product. Since the nature of land cover monitoring requires images of a different time, and change detection analysis is carried out most effectively with more than one image of a study area, three-time–series of the MODIS 13A1 data every 16 days at 500m spatial resolution as a gridded level–3 product in the Sinusoidal projection were acquired (i.e., for 2000, 2010, and 2020).

The product contains two principal vegetation layers (i.e., the Normalized Difference Vegetation Index [NDVI] and the Enhanced Vegetation Index [EVI]). The NDVI is a 'normalized' transformation of the NIR to RED reflectance ratio, ρNIR/ρRED, designed to standardize Vegetation Index (VI) values to between −1 and +1. It is based on the following equation.

$$\mathrm{NDVI} = \frac{\left(\frac{\rho\mathrm{NIR}}{\rho\mathrm{RED}}\right)}{\left(\frac{\rho\mathrm{NIR}}{\rho\mathrm{RED}}\right)} \qquad [1]$$

As a ratio, the NDVI has the advantage of minimizing certain types of the band–correlated noise and influences due to variations in direct/diffuse irradiance, clouds, and cloud shadows, sun and view angles, topography, atmospheric attenuation, calibration and instrument–related errors.

Data preparation

i. Pre–processing of the satellite data

MODIS datasets are typically delivered as HDF (hierarchical data format) 10 by 10 arc-degree– tiles projected in the Sinusoidal coordinate system. However, both HDF and Sinusoidal projected data require further processing to be compatible in different processing environments. Thus, the MODIS datasets were pre-processed to glue the tiles and coerce them into a more usable format. Then, they were projected from the Sinusoidal to WGS 1984 and converted to the GeoTIFF format. Furthermore, time series analysis of imageries requires that imageries of various years should overlap each other at the pixel level. Accordingly, the imageries were co-registered with minimal error. At this stage, all-time series imageries were made to completely overlap with each other.

ii. Mosaicking and resampling of MODIS datasets

As stated earlier, four tiles of MODIS 500m data covers the study area. Following the download and completion of all necessary preliminary preparations, the four tiles were mosaicked into a single image using the mosaicking tool. The parameter files (a list of files that must be adhered to) were generated. Furthermore, the dataset was subjected to resampling because only the values of the component covering the area of interest were used for the study instead of the full MODIS image. This is because when an image is reprojected to a different coordinate system, it usually has an image pixel grid in alignments other than the original image. Hence, the resampling process was used to reproject and cut the mosaic using the parameter file that resampled the image to the target coordinate

system (i.e., the local coordinate system). A value was computed for every pixel in the new image through sampling (interpolation) over a neighborhood of pixels from the conforming position in the original image. It is usually preferable to resample a given set of rasters to a specific image resolution and map projection before merging and analyzing them.

iii. Data sub-setting, index value, and determination of NDVI thres hold

We got the subset images of the study area by masking the boundary of the study area (Nigeria) from the mosaicked imageries to limit the ensuing analysis and enable quick processing (Okeke et al., 2008). MODIS-NDVI values provided by NASA data were multiplied by 10,000. Relative to the area of interest, the values however vary from 2000 to over 10,000. We maintained this range of value at the initial stage. Yet, multiplying the dataset by a scale factor (0.0001) converts the image values to the index values (-0.2 to 0.9). Additionally, we determined the NDVI threshold values that could distinguish between the different LULCs using ground verification data. For instance, NDVI values between 0.6 and 1.0 signify high vegetation. On the other hand, low vegetation and non-vegetation indicate lower values.

iv. Mapping and estimation of LULC in Nigeria

a. Image Classification

Image classification is one of the most effective approaches of processing satellite imagery (Srivastava et al., 2012). Various land cover features reflect the visible and infrared light in different ways (Navalgund, Jayaraman, and Roy, 2007). Image classification was used in this study to detect, identify, and classify the images of different features based on the actual classes they represent on the ground. The image classification can result in various thematic maps of the study area (Lillesand and Kiefer, 2000). Using the supervised classification method, we classified the imageries into six classes (see table 1) to create LULC maps. The SVM algorithms, which was used generally aims to achieve the optimal separating hyper plane that minimizes misclassifications. SVM incorporates kernel functions that translate the original object space into a higher dimensional space, giving the original object space nonlinear boundaries for data that is linearly inseparable. SVM is a commonly used algorithms in machine learning applications and has been widely applied to classify remote sensing data.

Table 1. LULC classes

Lulc	Description
Forest land	All land with woody vegetation that meets the criteria used to designate Forest Land falls into this category.
Cropland	Cropped land and agroforestry systems where the vegetation structure falls below the forests' thresholds.
Grassland	This includes rangelands and pasture land

	that are not considered Cropland. Also, lands with herbs and brushes, grassland from wildlands to recreational areas, and agricultural and silvi–-pastoral systems.
Wetlands	This includes areas of peat extraction and land that is saturated by water for all or part of the year (e.g., peatlands). It does not fall into other land–uses. It also includes reservoirs as managed subdivisions and natural rivers and lakes as unmanaged subdivisions.
Settlements	This includes all developed land of any size unless included under other categories.
Other lands	The LULC in this class includes bare soil, rock, ice, and all land areas that do not fall into other categories.

b. Ground truthing

Ground-truthing (field verification) is to certify that the information generated from an image is correct and truly represents the features on the ground. The classification accuracy does not depend on the classifier alone but also on the training and validation datasets (Pelletier et al., 2017), which can significantly influence estimates of land change (Pontius and Li, 2010). As a result, reference data from sources more precise and accurate than the classified data were used (Okeke and Karnieli, 2006); including a topographic map of Nigeria and the Google Earth image.

c. Classification accuracy assessment

Classification accuracy assessment is vital in image classification for the users to efficiently use the result (Okeke and Karnieli, 2006). The reason is that there is noclassification created from remote sensing data that can be completely accurate as errors originate from different sources including the classification algorithm itself. The two broad methods of assessing a classified image accuracy are the confusion (error) matrix and the Receiver Operating Characteristic (ROC) curve. We used the confusion matrix in this study. Here, information about accuracy assessment came in an error matrix. It shows the number of pixels attributed to a specific LULC class relative to the actual class on the ground (Foody, 2002).

The error matrix used in this study depended on independent reference datasets. Reference data can come from three sources including field surveys, finer-resolution images, and more accurately classified images or maps. In other words, reference data came from data sources assumed to be more accurate and precise than the data to be classified (Okeke and Karnieli, 2006). This study utilized reference data obtained from high-resolution images (Google Earth). The most significant elements in this table are user accuracy, producer accuracy, overall accuracy, and the kappa coefficients.

v. LULC change detection

Change detection employs various approaches in different application areas. The selection of appropriate technique depends on knowledge of the algorithms, the characteristics of the study area, and the accurate registration of the satellite input data. It may be categorized into two main groups: pre-classification and post-classification methods. The pre-classification change detection involves matching pixels for a pixel to process multi-date imageries of the same area to generate changes. The process in this case involve digitally matching and correlating the digital number (DN) of cells in a certain image with the DN value for the image of another time using change detection algorithm. The second method is the post-classification change detection. It is one of the most common change detection approaches, in which, the multi–temporal image of the same area is digitally classified. Several plusses are associated with this technique. It reduces sensor, atmospheric and environmental differences. The issue of normalizing between two dates in terms of atmospheric and sensor differences, is of course, lessened when data from two dates are classified independently. The post–classification method was used in this paper. After classifying the MODIS datasets and the accuracy assessment was carried out, two independent layers were overlaid. Through the use of pixel–by–the pixel comparison algorithm, the pixels that indicate changes between images were determined (Kohavi and Provost, 1998). In this way, changes were generated based on the classes rather than on differences in DN values.

In order to determine the gross losses and gains in area extent of each LULC class, a change detection algorithm was first applied to the two LULC maps (2000 and 2010), from which the relative net gains/losses in each LULC class were derived (Hussain, 2013). After processing the results, the outputs were divided by the initial LULC area extent, or the area extent in 2000. The relative net changes (gains and losses) as a percentage were calculated by multiplying the results by 100. The LULC maps of the years 2000 and 2010, 2010 and 2020 were the three combinations of LULC maps that were created here. The three periods of our LULC change analyses are represented by these three combinations.

The following "loss" or "gain" was used to describe a change in a particular LULC class during each period. A change in LULC class—for instance, LULC class A1 at time 1 to LULC class A2 at time 2—was classified as a transition from A1 to A2, or a loss in LULC class A1 and a gain in LULC class A2. We determined the gains and loss-es of the LULC classes in 2000–2010, and 2010–2020 based on this method. Additionally, the annual rate of change for each LULC class during each transition period was determined using Equation (1) below.

$$\text{Annual Rate of Change} = \frac{(\text{A2} - \text{A1})}{\text{A1}(\text{Y2} - \text{Y1})} \qquad [2]$$

where A1 represents each LULC class's initial area extent for each period in year 1 (Y1), and A2 represents each LULC class's final area extent in year 2 (Y2).

Results

Maps and estimates of land use/land cover in Nigeria

The result of image classification of each MODIS–NDVI data used in this study is the LULC estimates and maps depicting the six LULC categories of the study area as they were in 2000, 2010, and 2020 (see table 2 and fig. 2). The LULC maps in Figure 2 compare the conditions in Nigeria in 2000, 2010, and 2020 In essence, we saw the LULC categories expand and contract simultaneously.

Table 2. Areal extent (in sqkm) and percentages of LULC of Nigeria during the study epochs

Class	2000	%	2010	%	2020	%
Forest	132746.00	14.37	143189.80	15.50	151892.60	16.44
Grassland	255740.30	27.68	259247.10	28.06	251095.30	27.18
Cropland	202257.80	21.89	222534.30	24.09	203197.30	22.00
Other land	176302.30	19.09	175926.30	19.04	171789.10	18.60
Built–up	101034.80	10.94	91874.80	9.95	106198.30	11.50
Wetland	55683.50	6.03	30992.30	3.35	39592.05	4.29
Total	**923764.50**	**100**	**923764.60**	**100**	**923764.60**	**100**

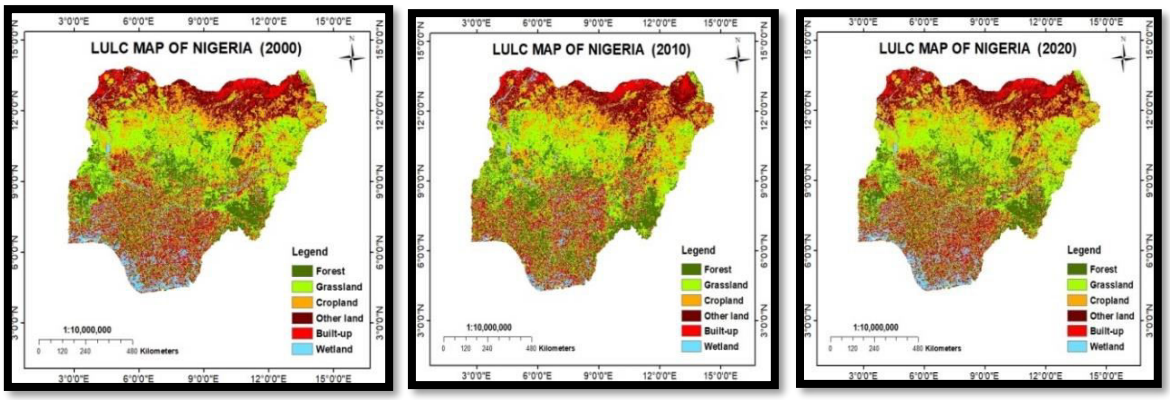

Figure 1. LULC map of Nigeria for the three epochs of study

The percentage coverage of the forest for 2000, 2010, and 2020 were 14.37, 15.55, and 16.44 respectively. The percentage coverage of the grassland for 2000, 2010, and 2020 were 27.68, 28.06, and 27.18 respectively. From the figures presented, it is obvious that grassland has the highest percentages throughout the time–series as compared to other classes of LULC. It recorded the highest percentage in 2010. Also, the percentage coverage

of the cropland for 2000, 2010, and 2020 were 21.89, 24.09, and 22.00 respectively. The percentage coverage of the other land for 2000, 2010, and 2020 were 19.09, 19.04, and 18.60 respectively. The percentage coverage of the built–up for 2000, 2010, and 2020 were 10.94, 9.95, and 11.50 respectively. The percentage coverage of the wetland for 2000, 2010, and 2020 were 6.03, 3.35, and 4.29 respectively.

Classification accuracy assessment results

The contingency table was used in this study for obtaining descriptive and analytical statistics of the LULC classification accuracy assessment (Okeke, Boroffice and Akinyede, 2008). In this case, they were used to summarize the information and also to obtain accuracy measures that can meet the present study goals (Smits, Dellepiane and Schowengerdt, 1999). The accuracy assessment results from the LULC classification for 2000, 2010, and 2020 are presented in table 3. The confusion matrix comprises the over-all accuracy, the user's and producer's accuracy, and various forms of kappa coefficients. The overall accuracy is the ratio of the sum of correctly classified pixels (i.e., the total amount of major diagonal entries) to the sum of pixels in the confusion matrix.

Table 3. Error matrix for 2000, 2010, and 2020 LULC classification

2000									
Class Value	**C_1**	**C_2**	**C_3**	**C_4**	**C_5**	**C_6**	**Total**	**U_Acc.**	**Kappa**
C_1	26	0	0	0	0	0	26	1.000	0
C_2	0	40	1	0	0	0	41	0.976	0
C_3	0	3	59	4	0	0	66	0.894	0
C_4	0	0	3	68	3	0	74	0.919	0
C_5	0	0	0	2	88	2	92	0.957	0
C_6	0	0	0	0	2	49	51	0.961	0
Total	26	43	63	74	93	51	350	0	0
P_Acc.	1	0.930	0.937	0.919	0.946	0.961	0	0.943	0
Kappa	0.000	0.000	0.000	0.000	0.000	0.000	0.000	0.000	0.929
2010									
Class Value	**C_1**	**C_2**	**C_3**	**C_4**	**C_5**	**C_6**	**Total**	**U_Acc.**	**Kappa**
C_1	18	0	0	0	0	0	18	1.000	0
C_2	0	31	7	0	0	0	38	0.816	0
C_3	0	2	58	6	0	0	66	0.879	0
C_4	0	0	1	73	7	0	81	0.901	0
C_5	0	0	0	1	85	7	93	0.914	0
C_6	0	0	0	0	0	55	55	1.000	0
Total	18	33	66	80	92	62	351	0.000	0
P_Acc.	1.000	0.939	0.879	0.913	0.924	0.887	0.000	0.912	0
Kappa	0.000	0.000	0.000	0.000	0.000	0.000	0.000	0.000	0.890

2020									
Class Value	**C_1**	**C_2**	**C_3**	**C_4**	**C_5**	**C_6**	**Total**	**U_Acc.**	**Kappa**
C_1	21	0	0	0	0	0	21	1.000	0
C_2	0	39	4	0	0	0	43	0.907	0
C_3	0	1	58	5	0	0	64	0.906	0
C_4	0	0	1	72	2	0	75	0.960	0
C_5	0	0	0	0	87	3	90	0.967	0
C_6	0	0	0	0	1	57	58	0.983	0
Total	21	40	63	77	90	60	351	0.000	0
P_Acc.	1.000	0.975	0.921	0.935	0.967	0.950	0.000	0.952	0
Kappa	0.000	0.000	0.000	0.000	0.000	0.000	0.000	0.000	0.940

Also, the summary statistics of accuracy assessment result in table 3 is presented in the table 4. Results in the table show that the overall accuracy obtained from the LULC classification for 2000, 2010, and 2020 were 94%, 91%, and 95%. Of course, these levels of accuracy are highly acceptable as they are higher than 85% stipulated by Anderson et al. (1996) as the required accuracy minimum for research of this nature.

Table 4. Summary of accuracy assessment result

Parameters	**2000**	**2010**	**2020**
Overall accuracy %)	94	91	95
Kappa	0.93	0.89	0.94

Furthermore, the kappa coefficient (K) is the percentage of correctly classified pixels extracted from the actual percentage expected by chance. The kappa coefficient has a value that varies between –1 and 1 but usually falls between 0 and 1. The kappa coefficients in this study were 0.93, 0.89, and 0.94 for 2000, 2010, and 2020 respectively. Of course, these values indicate an almost perfect correlation.

LULC Change detection results

The post-classification approach is the only method that results in a change that usually provides 'from – to' information (Okeke, Boroffice and Akinyede, 2008). In this study, the LULC changes were calculated between 2000 and 2010; and between 2010 and 2020 for the six LULC classes (see table 5).

Table 5. Change statistics over the study epochs 2000-2010

2000-2010			
Class	**Change**	**Annual Rate of Change**	**% Change**
Forest	10443.800	0.073	7.868

Grassland	3506.800	0.014	1.371
Cropland	20276.550	0.091	10.025
Other land	-375.950	-0.002	0.213
Built–up	-9159.950	-0.100	9.066
Wetland	-24691.200	-0.797	-44.342
2000-2010			
Class	**Change**	**Annual Rate of Change**	**% Change**
Forest	8702.800	0.057	6.078
Grassland	-8151.750	-0.032	-3.144
Cropland	-19337.000	-0.095	-8.689
Other land	-4137.250	-0.024	-2.352
Built–up	14323.500	0.135	15.590
Wetland	8599.750	0.217	27.748

The results in table 5 indicate that the highest increase in LULC between 2000 and 2010 occurred in forest land at 10443.800 sqkm (7.87 %) with an annual rate of change at 0.073. Also, the grassland increased between 2000 and 2010 at 3506.800 sqkm (1.37%) with an annual rate of change at 0.014. There was an increase in the cropland between 2000 and 2010 at 20276.550 sqkm (10.03%) with an annual rate of change at 0.091. For other lands, there was a decrease between 2000 and 2010 at 375.950 sqkm (0.21%) with an annual rate of change at 0.002. Also, the built–up shows a decreasing trend from 2000 to 2010 at 9159.950sqkm (9.07%) with an annual rate of change at 0.100. The wetland shows a decreasing trend from 2000 to 2010 at 24691.200 sqkm (44.34%) with an annual rate of change at 0.797. The decrease could be associated with land reclamation of the waterbodies, siltation and natural shrinkage in the volume of lakes and rivers. The effects are ecosystems and habitat loss, loss of livelihood, economic losses, in-creased poverty and settlement dislocation.

Furthermore, the forest cover increased by 8702.800 (6.08%) from 2010 to 2020 with an annual rate of change at 0.057. The grassland decreased from 2010 to 2020 at 8151.750 sqkm (3.14%) with an annual rate of change at 0.032. Of course, the decreases in grassland often result from agricultural activities and the increase is due to high gain from forest cover. The period between 2010 and 2020 recorded a decrease at 19337.000sqkm (8.69%) with an annual rate of change at 0.095. The other lands de-creased between 2010 and 2020 at 4137.250 sqkm (2.35%) with an annual rate of change at 0.024. The built–up increased between 2010 and 2020 at 14323.500sqkm (15.59%) with an annual rate of change at0.135. The wetland increased between 2010 and 2020 at 8599.750sqkm (27.75%) with an annual rate of change at 0.217. The in-crease in the wetland is mostly a result of an increase in rainfall and human imprint that allowed the water to persist on the forest cover that

gradually turned part of the forest cover into the wetland. Also, the percentage change in the LULC classes are presented in figure 3.

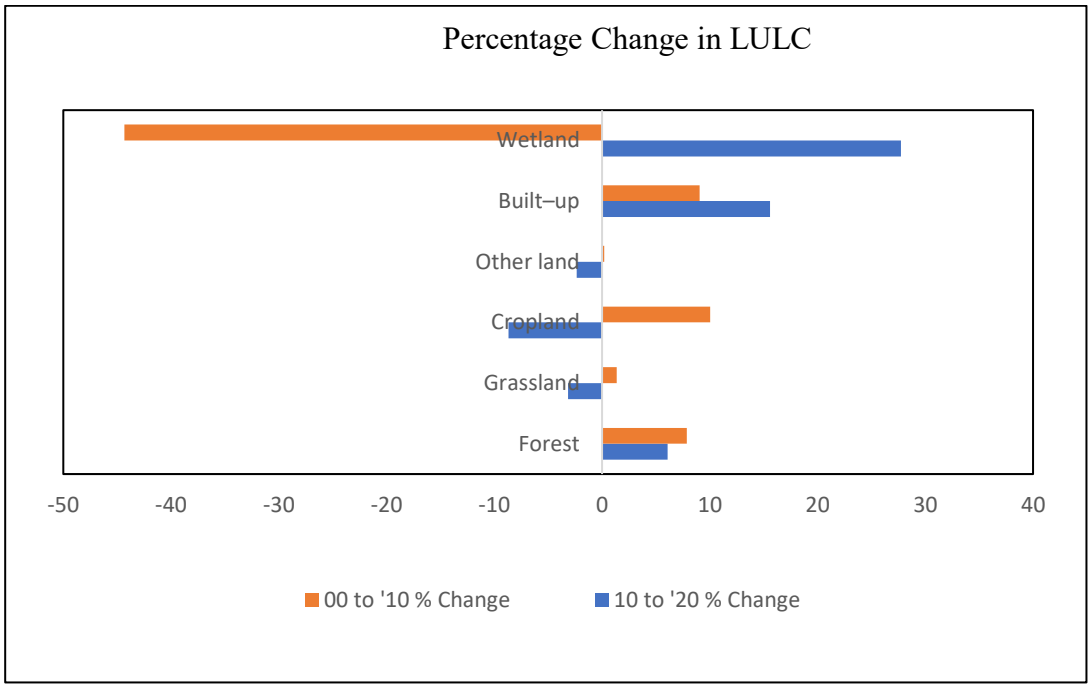

Figure 3. LULC map of Nigeria for the three epochs of study

The forest cover experienced a percentage change of 7.868 and 6.078 from 2000-2010 and 2010-2020 respectively. The implication is that despite the positive change or increase in the forest cover throughout the study epoch, the increase between 2010 and 2020 was slow compared to the earlier epoch. The grassland demonstrated a percentage increase of 1.371 from 2000 to 2010, but a percentage decrease of 3.144 from 2010 to 2020. This implied percentage gain and loss respectively. Also, the cropland increased by 10.025 percent between 2000 and 2010, and decreased by 8.689 percent from 2010 to 2020 indicating percentage gain and loss respectively. The other lands increased by 0.213 percent and decreased by 2.352 percent from 2000 to 2010 and from 2010 to 2020 respectively. Also, the built–up increased by 9.066 percent in period from 2000 to 2010 and further increased by 15.590 percent from 2010 to 2020. Finally, the wetland decreased by 44.342 percent and increased by 27.748 percent between 2000 and 2010, and between 2010 and 2020 respectively.

Conclusion

Using remote sensing data and GIS, we examined the scope, size, and character of LULC in Nigeria. We showcased three comprehensive wall-to-wall LULC maps and estimates of Nigeria at ten-year intervals, spanning 2000 to 2020. For the majority of land-cover classes, per-class producer and user accuracy was above 90%. This demonstrated the reliability of the estimates. Of course, this levels of accuracy obtained in the classification are highly acceptable as they are higher than 85% stipulated as the minimum ac-curacy required for research of this nature. Likewise, the kappa coefficients were 0.93, 0.89, and

0.94, for 2000, 2010, and 2020 correspondingly. This kappa coeffi-cients indicated an almost perfect correlation between the classified pixels and ground truth data.

The findings in this study indicated that LULC experienced fluctuating change during the period of study. There is significant variability regarding LULC in Nigeria. Depending on the requirements of the end users, the results from this study can be used in conjunction with other maps to build and apply post-processing rules. In a similar vein, these results can be utilized to pinpoint areas in need of further ground truth data.

This study proves the feasibility of mapping LULC time-series over extensive area using satellite data. To a significant extent, land dynamics may be understood using this paradigm for land change evaluation. The maps produced in this study offer a standardized data for evaluating land change at national, and local levels, as well as for use as inputs in other modeling projects and evaluations. Also, the study showed how current developments in GIS and its application for LULC analyses can be used to extract valuable earth surface information from long-term satellite data. Similarly, natural resources managers, policy makers, and other stakeholders will find the results of this study helpful for targeting and allocating resources and other land use interventions. However, future studies in this area should be focused on using various metrics inverifying that anthropogenic activities have intensified in tandem with the settlement growth this study has documented. It is also advised to test for statistical significance the main causes of the observed LULC change. Also, more research will relate this LULC change to time series population density data to confirm the observed human-induced LULC change.

Refrences

1. Abbas, Z., Jaber, H. S. (2020). Accuracy assessment of supervised classification methods for extraction land use maps using remote sensing and GIS techniques. IOP Conf. Series: Materials Science and Engineering, 745, 012166.
2. Adam, E., Mutanga, O., Odindi, J., and Abdel-Rahman, E. M. (2014). Land-use/cover classification in a heterogeneous coastal landscape using Rapid Eye imagery: Evaluating the performance of random forest and support vector machines classifiers. Int. J. Remote Sens., 35, 3440–3458.
3. Adeniyi, P. O. (1984). Land use and land cover inventory in Nigeria. Nig. Geogr. J., 27(1&2), 113–130.
4. Alexander, P., Brown, C., Arneth, A., Finnigan, J. and Rounsevell, M. D. A. (2016). Human appropriation of land for food: the role of diet. Global Environmental Change, 41, 88–98.
5. Anderson, J., Hardy, E., Roach, J., and Witmer, R. (1976). A land use and land cover classification sys-tem for use with remote sensor data (Washington: Government Printing Office)
6. Ardanuy, P. E., Han, D., and Salomonson, V. V. (1991). The Moderate Resolution Imaging Spectrometer (MODIS) science and data system requirements. IEEE Trans. Geosci. Remote Sens., 29(1), 75–88.

7. Balázs, B., Bíró, T., Dyke, G., Singh, S. K., Szabó, S. (2018). Extracting water-related features using reflectance data and principal component analysis of Landsat images. Hydrological Sciences Journal 63(2), 269–284.
8. Barnes, W. L., Xiong, X. and Salomonson, V. V. (2003). Status of Terra MODIS and Aqua MODIS. Advances in Space Research, 32(11), 2099–2106.
9. Bickel, K., Richards, G., Köhl, M. M., Leonardo, R., Rodrigues, V., and Stahl, G. (2006). Consistent representation of lands. 2006 IPCC Guidelines for National Greenhouse Gas Inventories.
10. Camargo, F. F., Sano, E. E., Almeida, C. M., Mura, J. C., and Almeida, T. A. (2019). Comparative assessment of machine-learning techniques for land use and land cover classification of the Brazilian tropical savanna using ALOS-2/PALSAR-2 polarimetric images. Remote Sens., 11, 1600.
11. Chen, Z., and Wang, J. (2010). Land use and land cover change detection using satellite remote sensing techniques in the mountainous Three Gorges Area, China. Int. J. Remote Sens., 31, 1519–1542.
12. Federal Ministry of Environment. (2001). National Action to Combat Desertification. Abuja, Nigeria: FME.
13. Foley, J. A., De Fries, R., Asner, G. P., Barford, C., Bonan, G., Snyder, P. K. (2005). Global consequences of land use. Sci., 309, 570–574.
14. Foody, G. M. (2002). Status of land cover classification accuracy assessment. Remote Sens. Environ., 80, 185–201.
15. Forestry Management and Coordinating Unit. (1996). Preliminary report on the assessment of land use and vegetation changes in Nigeria between 1978–1993/95. Submitted by Geometrics Interna-tional Inc. Canada: Ontario.
16. Güneralp, B., and Seto, K. (2013). Futures of global urban expansion: uncertainties and implications for biodiversity conservation. Environmntal Res. Lett., 8, 014025.
17. Heck, V., Hoff, H., Wirsenius, S., Meyer, C., and Kreft, H. (2018). Land use options for staying within the planetary boundaries – Synergies and trade-offs between global and local sustainability goals. Global Environmental Change, 2018, 49, 73–84.
18. Houghton, R. A. (2005). Aboveground forest biomass and the global carbon balance. Glob. Chang. Biol., 11, 945–958.
19. Hurtt, G. C., Chini, L. P., Frolking, S., Betts, R. A., Feddema, J., Wang, Y. P. (2011). Harmonization of land-use scenarios for the period 1500–2100: 600 years of global gridded annual land-use transitions, wood harvest, and resulting secondary lands. Clim. Chang., 109, 117.
20. Hussain, M., Chen, D., Cheng, A., Wei, H., and Stanley, D. (2013). Change detection from remotely sensed images: From pixel-based to object-based approaches. ISPRS J. Photogramm. Remote Sens., 80, 91–106.
21. Intergovernmental Panel on Climate Change. (2014). Climate Change, Contribution of Working Groups I, II and III to the Fifth Assessment Report of the Intergovernmental Panel on Climate Change. IPCC, Geneva, Switzerland.
22. Kohavi, R., and Provost, F. (1998). Guest Editors' Introduction: On applied research in machine learning. Machine Learning, 30, 127–132.

23. Lambin, E. F., Geist, H. J., and Lepers, E. (2003). Dynamics of land-use and land- cover change in tropi-cal regions. Annu. Rev. Environ. Resour., 28, 205–241.
24. Li, X., Chen, W., Cheng, X., and Wang, L. (2016). A comparison of machine learning algorithms for mapping of complex surface-mined and agricultural landscapes using ZiYuan-3 stereo satellite imagery. Remote Sens., 8, 514.
25. Lillesand, T. M., and Kiefer, R. W. (2000). Remote Sensing and Image Interpretation. John Wiley & Sons, New York.
26. Masuoka, E., Fleig, A., Wolfe, R.E. &Patt, F. (1998). Key characteristics of MODIS data products. IEEE Trans. Geosci. Remote Sens., 36(4), 1313–1323.
27. Maxwell, A. E., Warner, T. A., and Fang, F. (2018). Implementation of machine-learning classification in remote sensing: An applied review. Int. J. Remote Sens., 39, 2784–2817.
28. Mohammed, S. O., Gajere, E. N., Eguaroje, E. O., Shaba, H., Ogbole, J. O., Onyeuwaoma, N. D., and Ko-lawole, I. S. (2013). A spatiotemporal analysis of the national parks in Nigeria: A geoinformation approach. Ife J. Sci., 15(1), 159–166.
29. Navalgund, R. R., Jayaraman, V., and Roy, P. S. (2007). Remote sensing applications: An overview. Curr. Sci., 93(12), 1747-1766.
30. Ojha, A., Rout, J., Samal. R. N., Rajesh, G., Pattnaik. A. K., and Daspatnaik, P. (2013). Evaluation of land use/landcover dynamics of Chilika catchment. Int. J. Geom. Geosci., 4(2), 238–296.
31. Okeke, F. I., Boroffice, R. A., and Akinyede, J. (2008). Monitoring long term land use changes in Yankari National Park using Landsat and Nigeriasat–1 Data. Nig. J. Geogr. Environ., 1, 154– 169.
32. Okeke, F. I., and Karnieli, A. (2006). Methods for fuzzy classification and accuracy assessment of histor-ical aerial photographs for vegetation change analyses. Part I: Algorithm Development. Int. J. Remote Sens., 27(1), 153–176.
33. Okeke, F. I., and Omali, T. U. (2016). Spatiotemporal evaluation of forest reserves in the eastern region of Kogi state using geospatial technology. The Trop. Environ., 13 (1), 75–88.
34. Pelletier, C., Valero, S., Inglada, J., Champion, N., Marais Sicre, C., and Dedieu, G. (2017). Effect of training class label noise on classification performances for land cover mapping with satellite image time series. Remote Sens., 9, 173.
35. Peters, M. K., Hemp, A., Appelhans, T., Becker, J. N., Behler, C., Steffan-Dewenter, I. (2019). Climate–land-use interactions shape tropical mountain biodiversity and ecosystem functions. Nature, 568, 88–92.
36. Pontius Jr., R. G., Li, X. (2010). Land transition estimates from erroneous maps. Journal of Land Use Science, 5, 31–44.
37. Popp, A., Calvin, K., Fujimori, S., Havlik, P., Humpen¨oder, F., Vuuren, D. P. V. (2017). Land-use fu-tures in the shared socio-economic pathways. Global Environmental Change, 42, 331–345.
38. Rekha, P. N., Gangadharan, R., Ravichandran, P., Dharshini, S., Clarke, W., Pillai, S. M., Panigrahi, A., Ponniah, A. G. (2017). Land-use/land-cover change dynamics and groundwater quality in and around shrimp farming area in coastal watershed, Cuddalore district, Tamil Nadu, India. Curr. Sci., 113(9), 10, 1763-1770.

39. Scaioni, M., Longoni, L., Melillo, V., and Papini, M. (2014). Remote sensing for landslide investigations: An overview of recent achievements and perspectives. Remote Sens., 6, 9600–9652.
40. Shah, A. I., Sen, S., Din Dar, M. U., and Kumar, V. (2017). Land–Use/ Land–Cover change detection and analysis in Aglar watershed, Uttarakhand. Curr. J. Appl. Sci. Technol., 24(1), 1–11.
41. Smits, P. C., Dellepiane, S. G. and Schowengerdt, R. A. (1999). Quality assessment of image classification algorithms for land-cover mapping: a review and a proposal for a cost-based approach. Int. J. Remote Sens., 20, 1461–1486.
42. Soludo, C. (2006). Can Nigeria be China of Africa? A lecture delivered at the founders' day of the University of Benin, Benin City, Nigeria on November 23.
43. Song, X. -P., Hansen, M. C., Stehman, S. V., Potapov, P. V., Tyukavina, A., Vermote, E. F., and Townshend, J. R. (2018). Global land change from 1982 to 2016. Nature, 560, 639–643.
44. Srivastava, P. K., Han, D., Rico–Ramirez, M. A., Bray, M., & Islam, T. (2012). Selection of classification techniques for land use/land cover change investigation. Advance Space Research, 50, 1250–1265.
45. Teluguntla, P., Thenkabail, P. S., Oliphant, A., Xiong, J., Gumma, M. K., Congalton, R. G., and Huete, A. (2018). A 30-m Landsat-derived cropland extent product of Australia and China using random forest machine learning algorithm on Google Earth Engine cloud computing platform. ISPRS J. Photogramm. Remote Sens., 144, 325–340.
46. Turner, B. L., Lambin, E. F., and Reenberg, A. (2007). The emergence of land change science for global environmental change and sustainability. Proc. Natl. Acad. Sci., 104, 20666–20671.
47. Van Leeuwen, B., Tobak, Z., and Kovács, F. (2020). Machine learning techniques for land use/land cover classification of medium resolution optical satellite imagery focusing on temporary inundated areas. Journal of Environmental Geography 13 (1–2), 43–52.
48. Verburg, P. H., Crossman, N., Ellis, E. C., Heinimann, A., Hostert, P., Zhen, L. (2015). Land system science and sustainable development of the earth system: a global land project perspective. Anthropocene, 12, 29–41.
49. Viana, C. M., Girão, I., and Rocha, J. (2019). Long-term satellite image time-series for land use/land cov-er change detection using refined open source data in a rural region. Remote Sens., 11, 1104.
50. Wittke, S., Yu, X., Karjalainen, M., Hyyppä, J., and Puttonen, E. (2019). Comparison of two dimensional multi-temporal Sentinel-2 data with three-dimensional remote sensing data sources for forest inventory parameter estimation over a boreal forest. Int. J. Appl. Earth Obs. Geoinf., 76, 167–178.
51. Yousefi, S., Tazeh, M., Mirzaee, S., Moradi, H. R., and Tavangar, S. H. (2011). Comparison of different classification algorithms in satellite imagery to produce land use maps, case study: Noor city. J. Appl. RS GIS Tech. Nat. Res. Sci., 2, 15-25.
52. Zhang, C., Sargent, I., Pan, X., Li, H., Gardiner, A., Hare, J., and Atkinson, P. M. (2019). Joint Deep Learn-ing for land cover and land use classification. Remote Sens. Environ., 221, 173–187.